COMPARATIVE CORROSION STUDIES OF BRASS AND BRASS PLATED STEEL COINS

Cristiana Alexandra CRĂCIUN [1]

Coins gradually change in composition, shape, and appearance because of corrosion processes over time. This research aims to evaluate the influence of protective coating on the corrosion process of Romanian brass and brass-plated steel coins. This study looks at how brass and brass-plated steel corrode in saltwater solutions by using instruments such as scanning electron microscopy (SEM) in conjunction with energy dispersive X-ray spectroscopy (EDX) and electrochemical tests. Corrosion results revealed that after 744 h of exposure to this aggressive 3% NaCl environment, the difference between corrosion rate values is not that significant.

Keywords: coins, corrosion, electrochemical measurements

1. Introduction

Coins are valuable and reveal their architecture, society, and arts. Monarch, symbol, and inscribed emblems show political and economic history. Coin portrayals of famous buildings, temples, and other architectural marvels illustrate their time's art [1].

The materials of coins and their duration of circulation influence the degradation of their original appearance, coloration, and the clarity of surface pits [2]. Coins are made from metals or alloys with standardized designs. Due to their reduced cost and aesthetic appeal, nickel and copper alloys are used in coin manufacture most often. Nickel (Ni) is the most resistant metal but it is among the most hazardous metals, producing skin sensitivity and allergic reactions [3] the most prevalent of all contact allergies, being significantly elevated in the European population [4]. Once an individual develops a nickel allergy, a less quantity of nickel exposure to the skin is sufficient to induce allergic contact dermatitis compared to the initial amount required to trigger the allergy [4]. Since ancient times, coins have been made from brass, a binary Cu-Zn alloy. Orichalcum is an ancient word for a Cu-based alloy having 5–28% Zn like brass. This alloy was melted into ingots and utilized to make various things since it was more valuable than bronze [5]. Brass is extensively utilized in coins and heat

[1] * PhD Student, Dept. of General Chemistry, National University of Science and Technology POLITEHNICA Bucharest, Romania, * Corresponding author, e-mail danes.cristiana_alexandra@yahoo.com

exchangers due to its beautiful coloration. The tarnishing of currency is a prevalent occurrence during the circulation process. It decreases the lifespan of currency and diminishes the collectible worth of commemorative coins [2]. This also leads to the loss of significant knowledge (artistic, historical, scientific, social, etc.) [6]. The tarnishing of brass coinage can be attributed to various factors, including corrosive gases in the atmosphere and water molecules adsorbed on the surface. Coinage frequently meets skin during use, making sweat residue a primary cause of tarnishing [2]. Because corrosion makes it harder to keep private and public collections safe, a lot of science and technological work is being done to study how metals behave in corrosive environment [7].

Corrosion is a spontaneous, irreversible, and harmful physical-chemical deterioration of metals and alloys produced by mechanical, chemical, electrochemical, or biological environmental force, corrosion products having a very complex composition [8, 9]. Corrosion causes insoluble chemicals to develop in uneven and disturbed layers on the original surface [10]. The kind of metal, the nature and composition of alloying elements, the corrosive environment (including moisture content, pH levels, and salt), as well as pressure, temperature, and whether the environment is static or dynamic, influence corrosion [9, 11, 12]. Quantitative and qualitative methods can assess corrosion. Quality assessment usually involves visual inspection with a magnifying glass or microscope. Tests that create corrosion indices quantify corrosion damage [9]. Brass corrosion is complicated. Dezincification is the result of brass corrosion and may be caused by either a) selective Zn dissolution or b) dissolution of the two elements Cu and Zn accompanied by Cu re-deposition [5]. Because it is attacked by oxygen and hydrogen sulfide, copper does degrade. However, in the majority of cases, it may create a passivation layer or a solid corrosion barrier on the exterior of the item to prevent additional corrosion [13]. By creating a coating of copper metal, dezincing reduces the resistance of brass to corrosion, but when dezincing does not occur, copper corrosion products accelerate corrosion by autocatalysis [5]. Dezincification may occur in brasses with more than 15 wt.% Zn when exposed to corrosive water or soil environments [14]. Surface chemicals resulted during corrosion can be categorized as primary, secondary, or contaminant patina. The first patina, generated by copper oxides and Sulphur's, was later replaced by basic copper carbonates, with malachite serving both a protective and decorative purpose. The secondary patina forms during the final usage period due to hostile environmental variables, such as chloride anion in acidic environments and carbon dioxide in alkaline environments [15]. Dezincification dissolves brass-coated steels because Zn/Zn^{2+} has a lower redox potential than Cu/Cu^{2+} or Fe/Fe^{2+}. Copper galvanically corrodes steel and zinc. Copper surface enrichment from brass zinc depletion enhances galvanic coupling iron dissolution. The degrading process of brass-coated steel is influenced by environmental chemistry.

Dissolution kinetics are influenced by characteristics such as pH, oxygen level, and ionic force [16].

The corrosion mechanism and rate of copper alloys in seawater is a complex process affected by various factors, including: the manufacturing method, the presence of micro and macro structural weaknesses, the alloy's composition and heterogeneity, residual stresses, the object's microstructure, seawater salinity and corrosive agents, hydrodynamics and circulation temperature and pH of water, as well as the existence of oxygen and microbes, among other factors. The corrosion process is affected by the chemistry of corrosion byproducts, which encompasses The generation of various oxides, sulfides, carbonates, chlorides, and sulfates, in addition to the quality, density, and thickness of coatings [15]. Also, the corrosion behavior of wires made of brass-coated steel were studied in 1 M NaCl suggesting a corrosion model with two mechanisms: (a) general corrosion of brass due to zinc oxidation and zinc oxide/hydroxide formation, and (b) galvanic couplings between brass and iron accelerate steel oxidation in faulty zones, potentially causing detachment and wire breakage [17]. Galvanic interaction between steel and brass coating greatly influences brass-coated steel corrosion. The exact significance of the brass coating microstructure on the electrochemical reaction and corrosion behavior of brass-coated steel is not properly understood [18].

This study undertakes a comparative evaluation of the corrosion behavior of brass and brass-plated steel Romanian coins, employing advanced surface-analysis techniques and electrochemical methods. Using Tafel polarization and electrochemical impedance spectroscopy (EIS) in NaCl environments, the research elucidates the distinct corrosion mechanisms at play and uniquely investigates the potential for these coin types to form stabilizing, protective surface layers. To our knowledge, this detailed electrochemical and microstructural characterization of modern Romanian coins has not been previously documented in the corrosion literature.

2. Materials and Methods

For the evaluation tests of the time-dependent accelerated corrosion process, two sodium chloride aqueous solutions were prepared. The first solution contained 0.9% sodium chloride, while the second solution contained 3% sodium chloride. Studies were performed at room temperature. Circulating Romanian brass coins (having the following composition, according to quality certificate - Cu 81%; Zn 14%; Ni 5%, with 23,75 mm diameter) and circulating Romanian brass-plated steel coins (having the following composition, according to quality certificate, steel with a 98% Fe content coated with a Cu 99% layer ranging between 12 – 22 microns, followed by a Cu 67% Zn 33% layer ranging between

5.5 – 10.5 microns, having diameter of 16,75 mm), manufactured in the same year were used in this study. For all the tests, the coins were tested directly, without any pre-treatment or mechanical and chemical surface preparation. The only exception, to ensure a proper electrical contact for electrochemical tests, the coins were polished with abrasive paper to remove oxides. For the qualitative time-dependent characterization of the accelerated corrosion process, the Autolab PGSTAT 302N (Metrohm Autolab, B.V.) was used. The coins were subjected to comparative studies in different solutions. One brass coin and one brass-plated steel coin were immersed in NaCl 0.9% and studied for 24 h. Eight identical brass coins and eight brass-plated steel coins were immersed simultaneously in NaCl 3%. One coin of each type was used for measurements taken between the initial immersion and 24 hours, and another pair (one of each type) was used for measurements at 30 and 48 hours. The remaining six coins of each type were used for all subsequent measurements listed in Table 2, taken at 144, 216, 312, 408, 576, and 744 hours, respectively. The investigation continued in the NaCl 3% solution until 744 hours of immersion. The potentio-dynamic polarization approach was used to calculate the corrosion rate to quantitatively characterize the accelerated corrosion process in a time-dependent manner. Three electrodes were used in a homemade plexiglass electrochemical cell having an O ring at the bottom, which allowed only 0.5 cm^2 from samples surface to be exposed to the corrosive environment.

Thus, the following were used:

- Reference electrode (RE) Ag/AgCl, 3 M KCl, from Metrohm Autolab B.V; mounted at the top in a special support.
- Counter electrode (CE), Pt rod from Metrohm Autolab B.V; mounted at the top in a special support.
- Working electrode (WE): brass coin or brass-plated steel coin. As seen in Fig. 1 a, the WE was mounted at the bottom of the cell, with a metallic connector attached to a cable, and a yellow rubber seal prevented the liquid from leaking and ensured the controlled surface.

The potentio-dynamic polarization (Tafel plots) was acquired at 2 mV/sec between ± 300 mV and free potential. Using Nova software 1.11, the specific corrosion parameters were extracted. The electrochemical tests (OCP and Tafel polarization) were carried out following the general guidelines of ASTM G5-14 and ASTM G3-14 standards, which are commonly applied in corrosion research. Although no specific standard was strictly followed throughout the entire testing process, the methodology was adapted based on these references and on similar protocols in the literature [19]. With an AC potential amplitude of 10 mV, EIS measurements were carried out at free potential between 0.1 and 10^5 Hz. Data was also acquired and processed using Nova 1.11 software. One brass coin and one brass-plated steel coin were characterized before and after corrosion tests in NaCl

3% for 744 h. The samples were washed with distillated water and their surface was observed with a Nova NanoSEM 630 Scanning Electron Microscope equipped with EDX analyzer (FEI Company, Hillsboro, OR, USA). Grazing incidence X-ray diffraction (GI-XRD) investigations were carried out by using a 9kW Rigaku SmartLab diffractometer equipped with a CuKα1 source that provides a monochromatic beam with wavelength, λ = 0.1504 nm. The measurements were recorded in grazing-incidence mode, keeping constant the incidence angle at 0.5˚, while the detector moved from 10 to 95˚, with a scan speed of 5˚/min. One brass coin and one brass-plated steel coin were used for this study.

3. Results and discussion

The following graph from Fig. 1 b and c highlights the open circuit potential (OCP) of brass and brass-plated steel coins for one hour of exposure to a corrosive environment, while Fig. 1 d and f presents OCP values during first 30 h of immersion. In this study, the terms “OCP” (open circuit potential) and “Eoc” (electrode open circuit potential) are used interchangeably, both referring to the potential of the working electrode under open circuit conditions, without applied current.

It is observed (Fig. 1 b) that brass does not show large variations in the open circuit potential. In the case of brass-plated steel, its potential has more electronegative values than brass and shows various variations, but after 45 minutes its tendency is towards stabilization and passivation. In conclusion, in the first hour of immersion in 0.9% sodium chloride solution, brass was more stable. The graph presented in Fig. 1 c highlights the OCP of brass and brass-plated steel coins for one hour of exposure in a corrosive environment (3% sodium chloride). In the case of exposure to a more aggressive environment, it was observed that in the first 10 minutes of immersion, brass tends to passivate by shifting the potential to more positive values, while brass-plated steel shows a shift in the potential to more electronegative values. After this time, both samples tend to stabilize, brass at -0.18 V and brass-plated steel at -0.22 V. In conclusion, brass also shows a higher degree of stability than brass-plated steel.

Brass has different open circuit potentials in both environments. Thus, their values were more electronegative in 3% NaCl solution (more aggressive) and stabilization took longer. For brass-plated steel, the OCP are similar but more electronegative than for brass. It took longer for brass-plated steel to stabilize in NaCl 0.9% than in NaCl 3%. Fig. 1 d shows brass and brass-plated steel coins' OCP potential after 30 hours in NaCl 0.9%. It can be seen from the two curves that after 3 h of immersion in the corrosive environment, brass's OCP decreases toward higher electronegative values than brass-plated steel's. It gains value after

6 hours. Brass has higher electropositive OCP than brass-plated steel, as shown at the conclusion of the investigation. Fig. 1 e shows brass and brass-plated steel coins' OCP after 30 hours in NaCl 3%. Again, in a more severe corrosion environment, brass maintains a consistent and more electropositive potential than brass-plated steel, which fluctuates and becomes more electronegative.

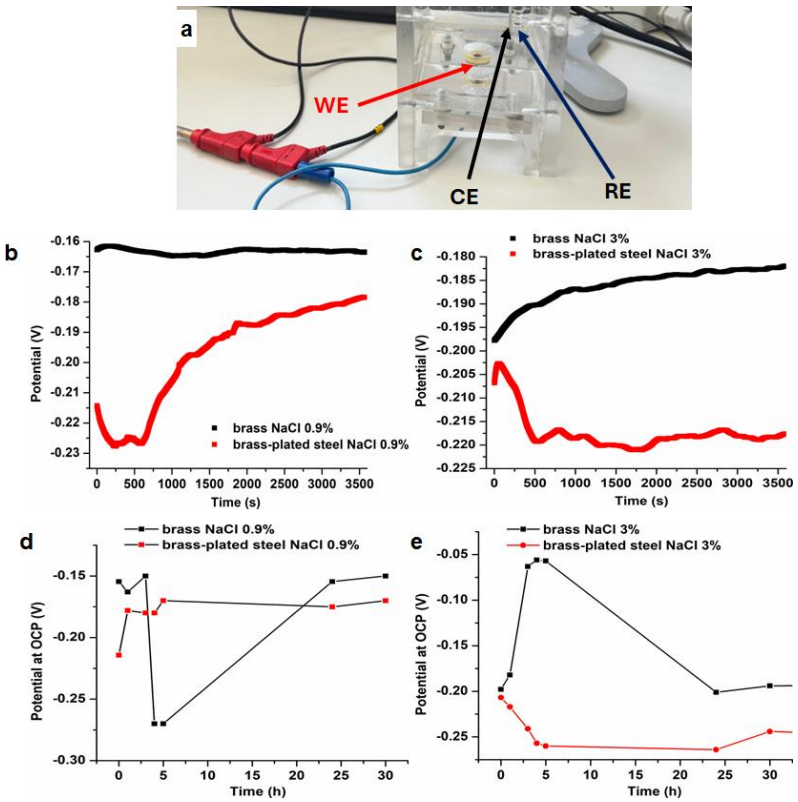

Fig. 1. a) The set up for electrochemical measurements; Brass and brass-plated steel coins' OCP for 1 h of exposure in NaCl: b) 0.9%, c) 3%; Potential at OCP during first 30 h of immersion in NaCl: d) 0.9%, and e) 3%;

In conclusion, in both environments, after 30 hours all samples have stabilized through passivation due to the formation of metal oxides on the surface. The transient processes (passivation / de-passivation) observed especially in the case of brass-plated steel suggest the formation of a more intense layer of oxides externally, in comparison to the brass specimen. Although both samples are resistant to corrosion, the visual appearance of the brass-plated steel samples is affected to a greater extent.

To gain more information and obtain the corrosion parameters, potentio-dinamic polarization was performed, and the obtained Tafel curve is presented in

Fig. 2. Tafel plots were recorded for brass and brass-plated steel at the first moment of exposure to a corrosive environment followed by the curves obtained after 24 hours of exposure to a corrosive environment. Fig. 2 a shows the results for NaCl 0.9% and Fig. 2 b, for NaCl 3%. Corrosion potential (E_{corr}) presents a more electropositive value at the beginning of immersion time in NaCl 0.9% for brass-plated steel compared to brass (Fig. 2 a). Following 24 hours of immersion, E_{corr} transitioned to a more negative value for brass-plated steel, whereas the anodic and cathodic curves exhibited an inclination towards elevated current densities. For brass, E_{corr} moved to higher positive values, and the anodic and cathodic curves exhibited a trend towards decreasing current densities, indicating passivation behavior after 24 hours. The cathodic curve for all samples displays a diffusion plateau between the potential range of −400 mV to −280 mV, which is documented in the literature as indicative of zinc corrosion product formation [20]. In a more corrosive environment (NaCl 3% - Fig. 2 b), E_{corr} shifted towards more negative values after 24 h of immersion, for both types of coins. Current densities do not have significant variations.

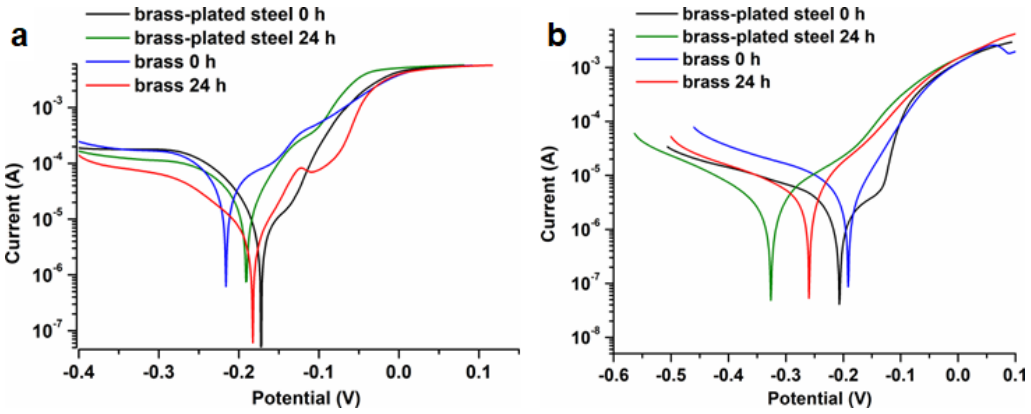

Fig. 2. Tafel plots for brass and brass-plated steel coins in: a) NaCl 0.9%, b) NaCl 3%

The corrosion rate, expressed in mm/year, was obtained using NOVA software based on the provided parameters, including equivalent weight, density, and surface area. The results are presented in Table 1. It is observed that after 24 hours the corrosion rate of brass is lower (0.014 mm/year) in NaCl 0.9% solution compared to the corrosion rate of brass-plated steel (0.033 mm/year). In NaCl 3%, the situation is reversed.

In literature there is contradictory information. A study has reported that the corrosion rate of iron and low-alloy steels in aerated water at ambient temperature peaks at approximately 3 wt% NaCl. Conversely, other investigations suggest that the maximum corrosion rate for carbon steel occurs at a lower concentration, around 1 wt% NaCl [21].

Because the corrosion rate after 24 hours of immersion in our case was elevated for both types of coins in the 3 % NaCl medium, the study was extended by an additional 744 hours under this more aggressive environment, in line with corrosion test protocols reported in comparable investigations [19].

Table 1

Corrosion rates from Tafel analysis

Material and Time	Corrosion rate [mm/year] NaCl 0,9% solution	Corrosion rate [mm/year] NaCl 3% solution
brass at initial time	0.105	0.065
brass at 24 h	0.014	0.089
brass-plated steel at initial time	0.017	0.041
brass-plated steel at 24 h	0.033	0.047

Fig. 3 shows the two coins' OCP variations in NaCl 3% over 744 h. Initial immersion hours showed a substantial positive potential change for brass sample. After 5 hours of immersion, the potential stabilized at -0.20 V. Cu(I), Cu (II) chloride or oxides, and Zn (II) oxides may cause this behavior. Brass-plated steel sample OCP shifts to a more negative value after 1h immersion. Following 24 hours of immersion, the potential stabilized at -0.25V. OCP for brass and brass-plated steel was practically the same after 576 h and achieved a steady state value of -0.22V. After 744 h, brass-plated steel's OCP decreased to -0.2V while brass's increased to -0.24V. Electrochemically, brass and brass-plated steel differed. Brass had steadier OCP, suggesting a passive layer. Brass-plated steel display temporal electrochemical potential fluctuations, suggesting complex activity. Copper oxide formation, oxide film breakage, and dezincification complicate this procedure.

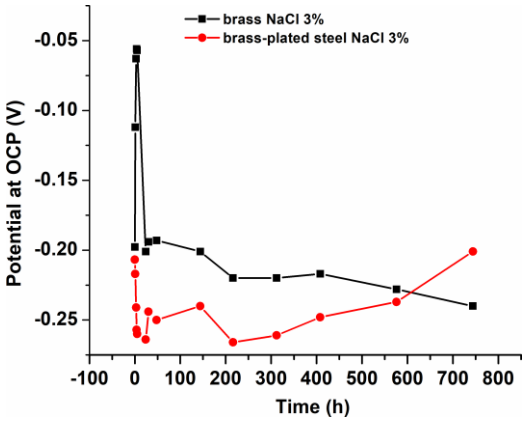

Fig. 3. OCP for the two coins samples in NaCl 3% during 744 h of corrosion

In Fig. 3 it's observed that brass-plated steel potential at initial time has the most electropositive value -0.2V. In the first hours, E_{corr} shifts to a more electronegative values, but after 5 h of immersion in NaCl 3% brass-plated steel it's showing a tendency to passivate. The behavior of brass-plated steel in the next days shows the formation of oxides along with the breakdown of oxide films. After 744 h the potential reached to potential of -0.3V. In Fig. 4 b it's revealed that brass potential of -0.2V at initial time. In the first hours the oxidation is evidenced by Tafel plots but after 5 h of immersion in NaCl 3% it's identified a more electropositive potential of -0.1V. Much passivation/de-passivation processes are evidenced in the next day's keeping a stable tendency. After 744 h the potential almost reaches -0.3V. In Fig. 4 c at initial time brass-plated steel has slightly more electronegative potential than brass has. The same situation is revealed after 744 h but the difference between the two samples remains insignificant.

Active-passive transitions occurred across all anodic polarization curves. Similar trends were seen in another research [21].

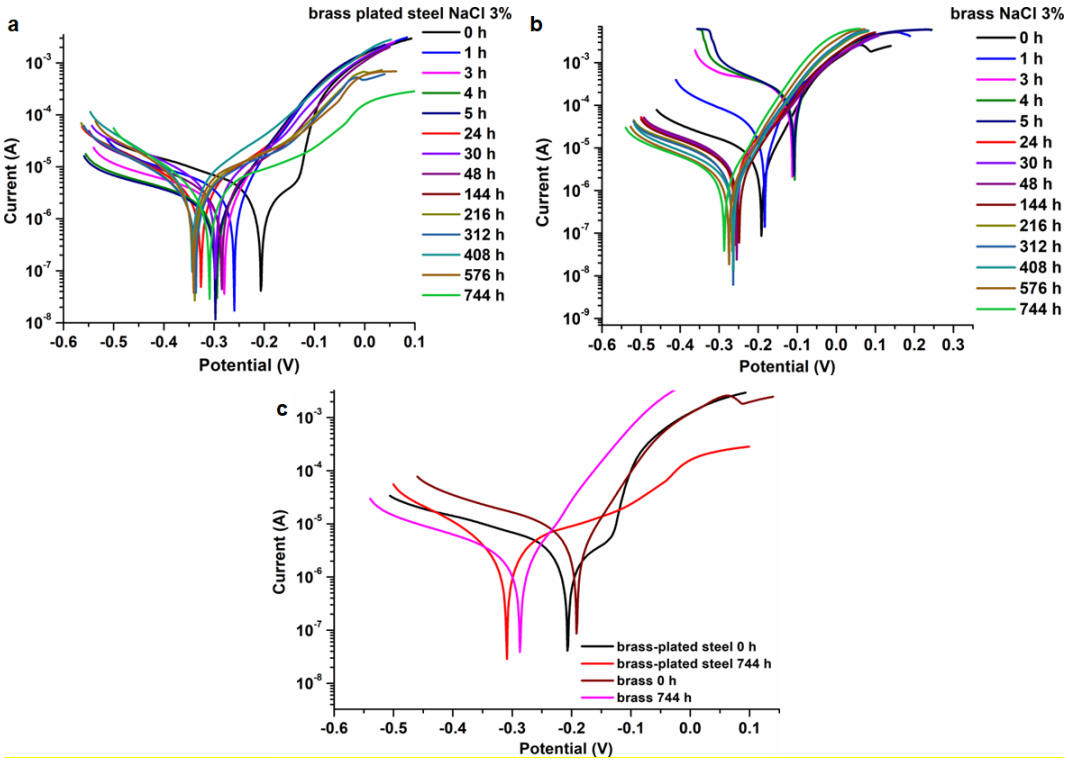

Fig. 4. Tafel slots of samples immersed in NaCl 3% from initial time until 744 h corresponding to: a) brass plated steel b) brass c) comparations of curves for the two coins samples

Both coin types had similar corrosion rates at initial time, as indicated in Table 2 and Tabel 3. The first five hours of brass corrosion are high, but after 24 hours it drops. Brass-plated steel corrosion fluctuates throughout the testing. Brass is less corrosion-prone than brass-plated steel after 744 hours of immersion, although the difference is small.

Table 2

Corrosion rates for brass during 744h of immersion in NaCl3%

Time	βa (V/dec)	βc (V/dec)	E_{corr} (V)	j_{corr} (A/cm²)	Corrosion rate (mm/year)
initial time	0.056554	0.10661	-0.18868	$5.3236 \cdot 10^{-6}$	0.065
1 h	0.098885	0.064981	-0.18265	$2.5062 \cdot 10^{-5}$	0.300
3 h	0.0951	0.19124	-0.1131	$2.793 \cdot 10^{-4}$	3.477
4 h	0.19475	0.086837	-0.10761	$2.652 \cdot 10^{-4}$	3.124
5 h	0.066996	0.11803	-0.10983	$1.817 \cdot 10^{-4}$	2.342
24 h	0.082256	0.2054	-0.25836	$7.1464 \cdot 10^{-6}$	0.089
30 h	0.087035	0.17209	-0.25434	$6.7756 \cdot 10^{-6}$	0.082
48 h	0.10131	0.18165	-0.25581	$7.2768 \cdot 10^{-6}$	0.088
144 h	0.065959	0.10663	-0.24814	$3.2316 \cdot 10^{-6}$	0.039
216 h	0.068257	0.048019	-0.26505	$1.9504 \cdot 10^{-6}$	0.023
312 h	0.067904	0.12562	-0.26299	$3.3116 \cdot 10^{-6}$	0.044
408 h	0.063468	0.10319	-0.2634	$2.2134 \cdot 10^{-6}$	0.030
576 h	0.062997	0.1263	-0.27325	$2.305 \cdot 10^{-6}$	0.028
744 h	0.061949	0.11986	-0.28506	$2.2796 \cdot 10^{-6}$	0.028

Table 3

Corrosion rates for brass-plated steel during 744h of immersion in NaCl3%

Time	βa (V/dec)	βc (V/dec)	E_{corr} (V)	j_{corr} (A/cm²)	Corrosion rate (mm/year)
initial time	0.14023	0.12471	-0.20282	$3.2878 \cdot 10^{-6}$	0.041
1 h	0.12511	0.066264	-0.24294	$3.8972 \cdot 10^{-6}$	0.048
3 h	0.066894	0.16251	-0.27818	$2.8288 \cdot 10^{-6}$	0.034
4 h	0.058236	0.11085	-0.2926	$1.5736 \cdot 10^{-6}$	0.019
5 h	0.050049	0.074047	-0.29731	$1.1107 \cdot 10^{-6}$	0.013
24 h	0.08685	0.12464	-0.32471	$3.8054 \cdot 10^{-6}$	0.047
30 h	0.13907	0.20471	-0.29777	$8.0484 \cdot 10^{-6}$	0.099
48 h	0.13681	0.076928	-0.28413	$3.38 \cdot 10^{-6}$	0.042
144 h	0.13724	0.17587	-0.30089	$5.3116 \cdot 10^{-6}$	0.066
216 h	0.13754	0.1607	-0.33903	$5.241 \cdot 10^{-6}$	0.064
312 h	0.15397	0.178	-0.33567	$5.4878 \cdot 10^{-6}$	0.068
408 h	0.14257	0.15013	-0.3429	$8.5728 \cdot 10^{-6}$	0.105
576 h	0.1748	0.14281	-0.34252	$7.1766 \cdot 10^{-6}$	0.088
744 h	0.1398	0.12411	-0.3091	$4.1558 \cdot 10^{-6}$	0.051

Figure 5 shows the SEM images for the two studied coins, before and after 744 h of immersion. Images from Fig. 5 e, f, g and h demonstrated that the two coins had a rough, non-homogeneous surface with irregular relief, micro-fissures, and mineral deposits after 744 h of exposure to NaCl 3%. The brass-plated steel coin has a more porous corrosion layer (Fig. 5 f) compared to brass coin (Fig. 5 h) indicating a higher degree of corrosion in the external layer.

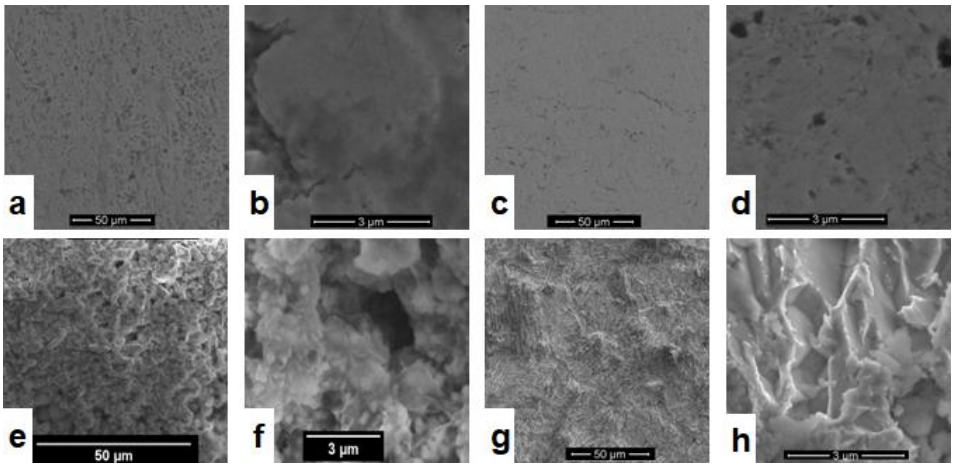

Fig. 5. SEM images for control samples: a), b) brass-plated steel coin; c) d) brass coin; and coins after 744 h of exposure to NaCl 3%: e), f) brass-plated steel coin; g), h) brass coin

In Fig. 6 a and c for brass-plated steel, the % of Zn may not be seen owing to the thin brass layer (5.5–10.5 microns) but associated oxide development on the copper surface and dezincification. Zn% is higher than the controlled sample probably because ZnO appears on brass surface after 744 h in NaCl 3% (Fig. 6 b). The dissolution-deposition hypothesis asserts that Cu and Zn dissolve simultaneously, eventually resulting in the redeposition of copper at a suitable level, culminating in a Cu layer with a complex composition and structure [22]. Research on various brass alloys exposed to corrosion [22], it was shown that an increase in copper content within the alloy, enhanced the brass alloys' capacity to withstand detrimental surrounding ions. After 744 hours in a corrosive environment, the control sample's copper content drops by 50% at the coin surface (Fig. 6 d). This tendency was also observed in other study [22]. Literature [23] indicates that brass susceptibility to sulfate and chloride corrosion, which alters the oxide layer formed, is the underlying cause of this phenomenon.

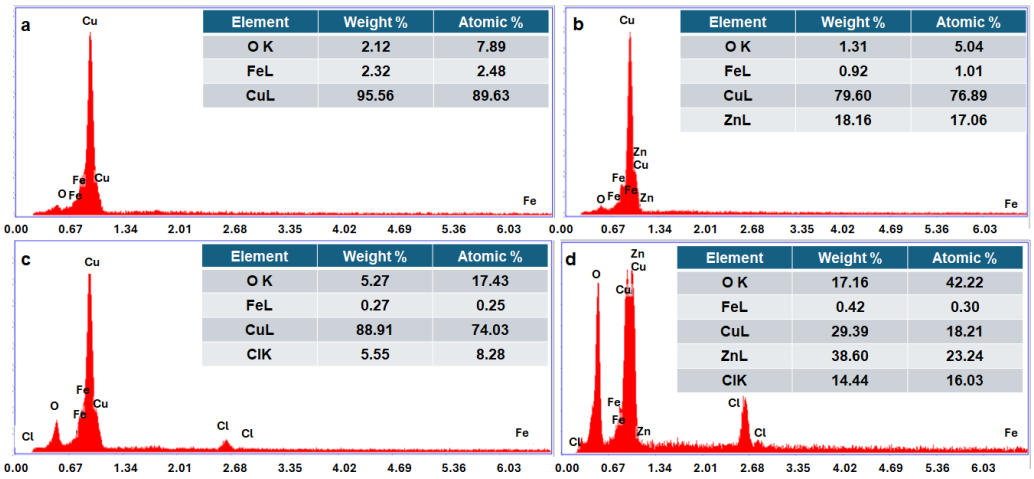

Fig. 6. EDX result of coins: a) brass-plated steel coin – control sample; b) brass coin– control sample; c) brass-plated steel coin after 744 h of immersion in NaCl 3%; d) brass coin after 744 h of immersion in NaCl 3%

Fig. 7 a and b, shows normalized Nyquist graphs for both types of coins, recorded at OCP. For any of samples, the Nyquist diagram does not exhibit a perfect semicircle; this is attributed to frequency dispersion caused by surface roughness [24], also, this signifies the presence of capacitive behavior [25]. Corrosion resistance rises with capacitive loop size. Brass capacitive loop increased after 744 h, as seen in Fig. 7 c. After 744 h, brass-plated steel shapes remain consistent. Brass exhibited the shortest capacitive loop at initial time, indicating the lowest corrosion resistance. The analogous circuit utilized to fit the data is represented in Fig. 7 d. The circuit used to fit the data is a modified Randles circuit like the circuit used in the literature for brass corrosion [26]. The resistance R_s considers resistance from NaCl 3% corrosive environment. A resistance (R_1) was applied with a constant phase element (CPE_1) for the oxide layer formed during the passivation/depasivation mechanisms, visible also in SEM images (Fig. 5 e, f, g and h). Another resistance (R_2) in parallel with a constant phase element (CPE_2) was added to consider the barrier oxide layer present on every metal surface in contact with air and visible in SEM image from Fig. 5 a, b, c and d.

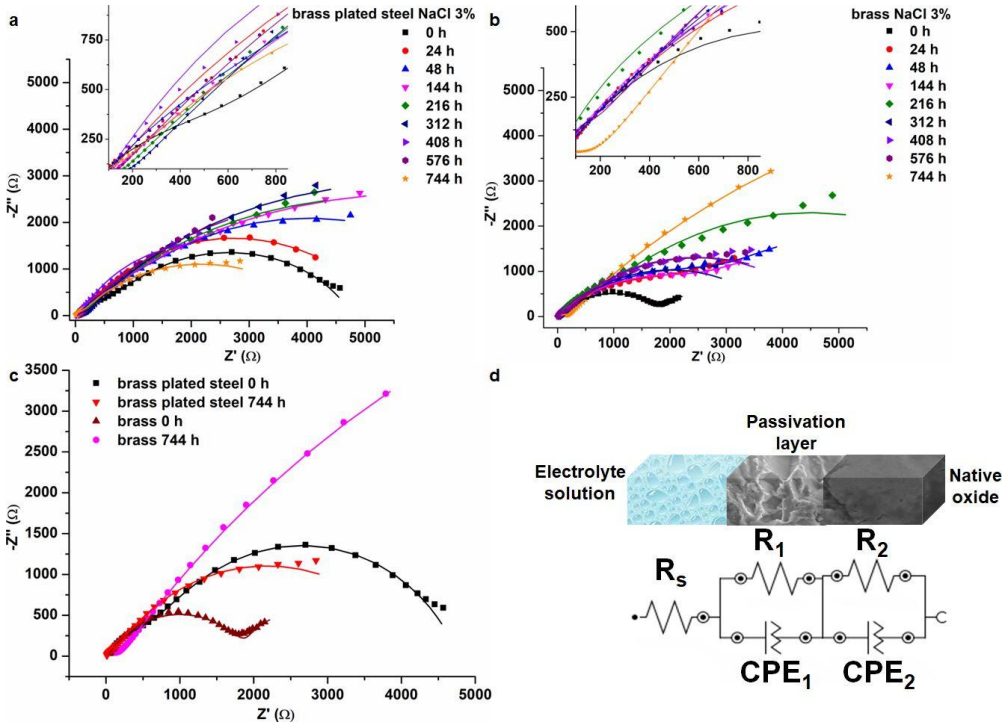

Fig. 7. EIS, Nyquist plot of samples immersed in NaCl 3% from initial time until 744 h corresponding to: a) brass plated steel b) brass c) comparations of curves for the two coins samples; and d) corresponding circuit used to fit the data.

The electrical parameters acquired using the Nova software are displayed in Table 4 and 5. Because the saline solution (NaCl 3%) and testing conditions are similar (room temperature and light), the solution resistance of all the samples that were evaluated is approximately between 10 - 50 Ω. CPE is defined by Y_0 and N, the ideal capacitance admittance and empirical constant, respectively. The values of the empirical constant N_1 and respective N_2 range from 0 to 1. The deviation from theoretical capacitance is represented by the exponential component N in the CPE equation. With Y_0 equal to R, the CPE displays properties like those of a pure resistor when N is equal to 0. In contrast, the CPE acts as a pure capacitor when N equals 1. Based on the N values, which range from 0.5 to 0.99 in most cases, it is feasible to deduce that all tested coins have a pseudocapacitive character. χ^2 values ranged from 10^{-2} to 10^{-3}, indicating satisfactory circuit fit.

Table 4 shows that resistance R_1 is continuously increasing from initial time of immersion up to 144 h, reaching the highest value. After 144 h, the trend oscillates continuously, and after 744 h, it is one order of magnitude lower than initial time. From $4 \cdot 10^3$ Ω·cm^2 to $12 \cdot 10^3$ Ω·cm^2, resistance R_2 does not vary much. After 744 h of immersion, R_2 mimics the value for initial time.

Table 5 shows that the resistance remains elevated throughout the entire measurement process, greater compared to brass plated steel. This correlates well with the SEM images that reveal a significantly more compact passivation layer in the case of brass compared to brass-plated steel. Resistance R_1 decreased with one order of magnitude. Resistance R_2 increased from $1.928 \cdot 10^3$ $\Omega \cdot cm^2$ to $21.778 \cdot 10^3$ $\Omega \cdot cm^2$.

Table 4

Electrical characteristics derived from the fitted EIS data corresponding to brass-plated steel coin

Brass-plated steel sample	Parameter							
	R_s ($\Omega \cdot cm^2$)	R_1 ($\Omega \cdot cm^2$)	CPE_1		R_2 ($\Omega \cdot cm^2$)	CPE_2		χ^2
			Y_{o1} ($S \cdot s^n$)	N_1		Y_{o2} ($S \cdot s^n$)	N_2	
initial time	31.98	599.52	$2.12 \cdot 10^{-5}$	0.69	$4.15 \cdot 10^3$	$6.33 \cdot 10^{-5}$	0.73	0.007
24 h	53.02	849.95	$106 \cdot 10^{-5}$	0.99	$4.59 \cdot 10^3$	$21.74 \cdot 10^{-5}$	0.64	0.021
48 h	45.55	801.40	$21.99 \cdot 10^{-5}$	0.65	$6.64 \cdot 10^3$	$26.19 \cdot 10^{-5}$	0.70	0.012
144 h	37.93	899.73	$5331 \cdot 10^{-5}$	0.85	$11.35 \cdot 10^3$	$19.89 \cdot 10^{-5}$	0.54	0.013
216 h	39.91	58.61	$5.40 \cdot 10^{-5}$	0.71	$10.47 \cdot 10^3$	$24.97 \cdot 10^{-5}$	0.58	0.011
312 h	34.95	113.14	$4.09 \cdot 10^{-5}$	0.67	$11.17 \cdot 10^3$	$25.77 \cdot 10^{-5}$	0.60	0.009
408 h	36.38	618.47	$569 \cdot 10^{-5}$	0.48	$3.91 \cdot 10^3$	$296 \cdot 10^{-5}$	0.81	0.040
576 h	26.87	134.63	$436 \cdot 10^{-5}$	0.20	$9.71 \cdot 10^3$	$47.26 \cdot 10^{-5}$	0.61	0.032
744 h	27.37	76.20	$4.17 \cdot 10^{-5}$	0.92	$4.18 \cdot 10^3$	$27.57 \cdot 10^{-5}$	0.62	0.030

Table 5

Parameters for suggested equivalent circuits corresponding to brass coins

Brass sample	Parameter							
	R_s ($\Omega \cdot cm^2$)	R_1 ($\Omega \cdot cm^2$)	CPE_1		R_2 ($\Omega \cdot cm^2$)	CPE_2		χ^2
			Y_{o1} ($S \cdot s^n$)	N_1		Y_{o2} ($S \cdot s^n$)	N_2	
initial time	25.84	1012.1	$2154 \cdot 10^{-5}$	0.93	$1.93 \cdot 10^3$	$7.55 \cdot 10^{-5}$	0.62	0.042
24 h	26.79	2073.1	$983 \cdot 10^{-5}$	0.94	$2.90 \cdot 10^3$	$38.44 \cdot 10^{-5}$	0.59	0.016
48 h	18.74	2844.4	$1031 \cdot 10^{-5}$	0.95	$3.85 \cdot 10^3$	$27.70 \cdot 10^{-5}$	0.57	0.042
144 h	14.86	2728.8	$593 \cdot 10^{-5}$	0.87	$3.18 \cdot 10^3$	$22.54 \cdot 10^{-5}$	0.59	0.035
216 h	15.62	868.99	$10.63 \cdot 10^{-5}$	0.75	$7.39 \cdot 10^3$	$23.78 \cdot 10^{-5}$	0.70	0.078
312 h	12.79	80.853	$10.21 \cdot 10^{-5}$	0.87	$3.84 \cdot 10^3$	$23.69 \cdot 10^{-5}$	0.63	0.049
408 h	16.09	145.99	$6.16 \cdot 10^{-5}$	0.86	$4.59 \cdot 10^3$	$21.56 \cdot 10^{-5}$	0.66	0.097
576 h	10.34	103.34	$4.63 \cdot 10^{-5}$	0.91	$4.81 \cdot 10^3$	$23.26 \cdot 10^{-5}$	0.63	0.049
744 h	7.61	155.37	$6.37 \cdot 10^{-5}$	0.48	$21.78 \cdot 10^3$	$32.96 \cdot 10^{-5}$	0.57	0.005

For brass-plated steel coin (Fig. 8 a), one can observe the presence of diffraction peaks at 2θ = 42.8, 50.3, 73.5, 89.1°, which could be assigned as different reflections of Cu-Zn alloys [27, 28]. After corrosion process, one can note the presence of additional small diffraction features at 2θ = 15.4, 31.6, 34.14,

36.2, 56.6, 62.8˚ that were further assigned for the corrosion products of brass, mostly consisting of Cu_2O (cuprite) and CuO, along with minor quantities of $Cu_2Cl(OH)_3$ (atacamite), ZnO (zincite) [28-30] and $NaClO_3$ compound (card no. 70-0471).

The brass coin (Fig. 8 b) exhibits diffraction peaks at 2θ = 42.8, 50.3, 73.5, and 89.1˚, which may be attributed to various reflections of Cu-Zn alloys [27, 28]. Subsequent minor diffraction patterns at 2θ = 15.4, 31.6, and 36.2˚ were attributed to the corrosion process, specifically identifying the corrosion products of brass, predominantly comprising Cu_2O (cuprite) and CuO, alongside trace amounts of $Cu_2Cl(OH)_3$ (atacamite) and ZnO (zincite), [28-30] as well as the $NaClO_3$ compound (card no. 70-0471).

Conductivity and pH measurements were conducted on the original solution as well as on the solutions in which the two coins had been immersed for 744 hours. Brass-plate steel conductivity increases from 45.9 mS/cm to 135.2 mS/cm after 744 h, indicating higher ion release. Brass has an order of magnitude lower conductivity (46.8 mS/cm) than brass-plated steel because it releases fewer ions into the solution. Brass pH was 5.9 and brass-plated steel 6.9 after 744 hours, both close to 6 (the initial pH value).

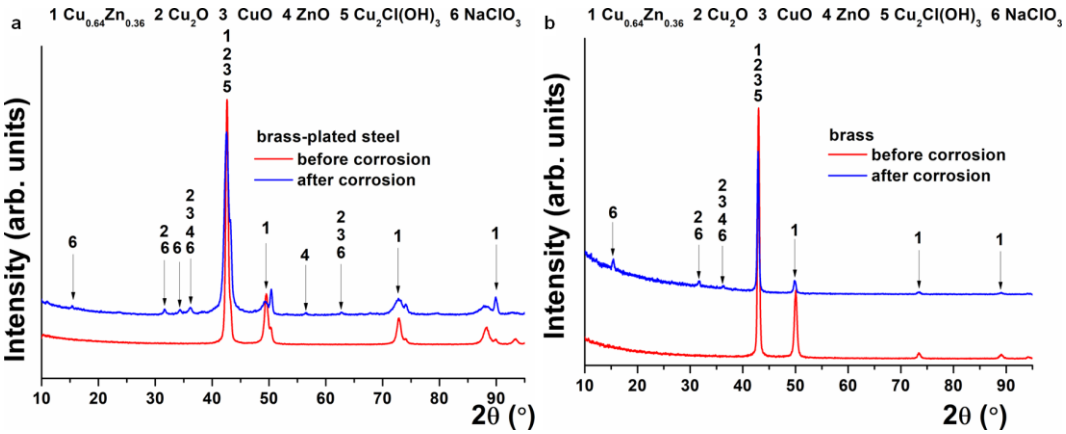

Fig. 8. Grazing incidence X-ray diffraction spectra before and after 744 h of corrosion in NaCl 3% for: a) brass-plated steel coin; b) brass coin

4. Conclusions

Comparative studies were performed to evaluate accelerated corrosion over time on brass and brass-plated steel coins, in different concentrations of salt solutions (NaCl 0.9%, and NaCl 3%). Brass presents differences in the open circuit potential values between the two environments, showing more electronegative values in the more aggressive solution (NaCl 3%), along with a

longer stabilization time. In contrast, brass-plated steel shows similar open circuit potential values across both environments, although these values are more electronegative compared to those of brass.

Tafel plots show that brass-plated steel has slightly more electronegative potential than brass has. The same situation is revealed after 744 h of immersion in NaCl 3% but the difference between the two samples remains insignificant. At the same time, the calculation of corrosion rates highlighted the fact that after 744 hours of immersion in NaCl 3%, brass demonstrates a lower susceptibility to corrosion compared to brass-plated steel, although the difference is not substantial. SEM images/EDX revels that both samples formed oxides on the surface that led to their stabilization in the corrosive environments studied, but it was observed a significantly more compact passivation layer in the case of brass compared to brass-plated steel, which indicates a higher degree of corrosion in the external layer of brass-plated steel. The resistance from EIS measurements stays consistently high for brass coin over the whole measuring procedure, surpassing that of brass-plated steel coin.

Given similar corrosion resistance, brass-plated steel may offer a cost-effective alternative to solid brass, especially considering the lower material cost. However, potential long-term durability, manufacturing complexity, and coating integrity should be carefully evaluated when selecting the appropriate material for coin production.

Acknowledgment

The author extends their appreciation to the following researchers which were providing guidance, assistance and technical support for this work: Prof. Dr. Cristian Pirvu (UNSTPB), Ş.L. Dr. Cristina Dumitriu (UNSTPB), Dr. Oana Brîncoveanu (IMTB) and Dr. Cosmin Romaniţan (IMTB).

R E F E R E N C E S

1. *S. M. Saleh, A. E.-H. A. El-Badry, A. M. Abdel-karim*, Evaluation of the corrosion resistance of bronze patina or/and protective coating on the surface of the archaeological coins, Sci. Rep., Vol. **15**, 2025, DOI: 10.1038/s41598-025-85290-x.
2. *L. Z. Mohamed, A. M. Elzohry, L. A. Khorshed, A. Attia, M. A. Adly*, Corrosion Behavior of Coins in Artificial Sweat Solution: A Review, Int. J. Electrochem. Sci., Vol. **17**, 2022, DOI: 10.20964/2022.01.17.
3. *A. M. Elzohry, L. A. Khorshed, A. Attia, M. A. Adly, L. Z. Mohamed*, Chemical, Electrochemical and Corrosive Wear Behavior of Nickel-plated Steel and Brass-plated Steel Based Coins from Egypt in Artificial Sweat, International Journal of Electrochemical Science, Vol. **16**, 2021, DOI: 10.20964/2021.08.33.
4. *L. Reclaru, C. M. Cotrut, D. M. Vranceanu, F. Ionescu*, Evaluation of Galvanic and Crevice Corrosion of Watch Case Middle (1.4435 Steel) and Bottom (Panacea® Steel) Assembly

Supposed to Be in Prolonged Contact with the Skin, Coatings, Vol. **13**, 2023 DOI: 10.3390/coatings13050943.
5. *M. Di Fazio et al.*, Solid-state electrochemical characterization of emissions and authorities producing Roman brass coins, Microchem. J., Vol. **152**, 2020, DOI: 10.1016/j.microc.2019.104306.
6. *G. A. Mahmoud, S. M. Saleh, A. Abdel-karim, A. El-Meligi*, The influence of urban sprawl on corrosion rate of buried archaeological coins, Shedet, Vol. **13**, 2024, DOI: 10.21608/shedet.2024.366930.
7. *M. Di Fazio, A. C. Felici, F. Catalli, L. Medeghini, C. De Vito*, Micro and nanoscale structures and corrosion patterns in brass: the case study of ancient roman orichalcum coins, Minerals, Vol. **12**, 2022, DOI: 10.3390/min12070827.
8. *I. Sandu, C. Marutoiu, I. Sandu, A. Alexandru, A. Sandu*, Authentication of old bronze coins I. Study on archaeological patina, Acta Univ. Cibiniensis Seria F Chemia, Vol. **9**, 2006.
9. *P. Popoola*, Corrosion Resistance Through the Application of Anti- Corrosion Coatings. (Developments in Corrosion Protection), IntechOpen, Rijeka, 2014.
10. *O. Papadopoulou, P. Vassiliou, S. Grassini, E. Angelini, V. Gouda*, Soil-induced corrosion of ancient Roman brass – a case study, Mater. Corros., Vol. **67**, 2016, DOI: 10.1002/maco.201408115.
11. *F. Boccaccini et al.*, Early stages of metal corrosion in coastal archaeological sites: effects of chemical composition in silver and copper alloys, Materials, Vol. **17**, 2024, DOI: 10.3390/ma17020442.
12. *M. Abdelbar, A. M. El-Shamy*, Understanding soil factors in corrosion and conservation of buried bronze statuettes: insights for preservation strategies, Sci. Rep., Vol. **14**, 2024, DOI: 10.1038/s41598-024-69490-5.
13. *H. Huisman et al.*, Change lost: Corrosion of Roman copper alloy coins in changing and variable burial environments, J. Archaeol. Sci. Rep., Vol. **47**, 2023, DOI: 10.1016/j.jasrep.2022.103799.
14. *V. Gerstner, R. Bureš, J. Stoulil*, Electroless brassing of historical artefacts, Koroze a Ochrana Materiálu, Vol. **68**, 2024, DOI: 10.2478/kom-2024-0001.
15. *A. Gharib*, A scientific study of the patina, corrosion morphology, and conservation of egyptian brass object, EJARS, Vol. **4**, 2014, DOI: 10.21608/ejars.2018.7271.
16. *A. Romaine et al.*, Importance of the surface and environmental conditions on the corrosion behavior of brass, steel and brass coated steel wires and brass coated steel cords, Corros. Sci., Vol. **177**, 2020, DOI: 10.1016/j.corsci.2020.108966.
17. *S. Chanel, N. Pébère*, An investigation on the corrosion of brass-coated steel cords for tyres by electrochemical techniques, Corros. Sci., Vol. **43**, 2001, DOI: 10.1016/S0010-938X(00)00093-7.
18. *V. Vignal, V. Rault, H. Krawiec, A. Lukaszczyk, F. Dufour*, Microstructure and corrosion behaviour of deformed pearlitic and brass-coated pearlitic steels in sodium chloride solution, Electrochim. Acta, Vol. **203**, 2016, DOI: 10.1016/j.electacta.2016.03.005.
19. *H. Wang et al.*, The effect of lead content on stress corrosion behavior of brass, Corros. Sci., Vol. **245**, 2025, DOI: 10.1016/j.corsci.2025.112714.
20. *N. Ben Seddik et al.*, Computational, theoretical and experimental studies of four amino acids as corrosion inhibitors for brass in 3% NaCl medium, J. Mol. Liq., Vol. **397**, 2024, DOI: 10.1016/j.molliq.2024.124113.
21. *F. Brownlie, T. Hodgkiess, A. Pearson, A. Galloway*, Electrochemical Evaluation of the Effect of Different NaCl Concentrations on Low Alloy- and Stainless Steels under Corrosion and Erosion-Corrosion Conditions, Corros. Mater. Degrad., Vol. **3**, 2022, DOI: 10.3390/cmd3010006.

22. *Z. Liang, K. Jiang, T.-a. Zhang, S. Lin*, Corrosion behavior of brass from the Western Zhou Dynasty in an archeological-corrosive medium, J. Alloys Compd., Vol. **865**, 2021, DOI: 10.1016/j.jallcom.2020.158579.
23. *R. Lachhab et al.*, Comparative study of the corrosion behavior of three alpha brass alloys used in potable water distribution equipment in aggressive soil using electrochemical measurements, Ceram. Int., Vol. **50**, 2024, DOI: 10.1016/j.ceramint.2023.10.185.
24. *A. Fouda, R. Ahmed, A. El-Hossiany*, Chemical, electrochemical and quantum chemical studies for famotidine drug as a safe corrosion inhibitor for α-brass in HCl solution, Prot. Met. Phys. Chem. Surf., Vol. **57**, 2021, DOI: 10.1134/S207020512101010X.
25. *S. Ganguly, R. Gope, M. A. Kamde, S. Pahari, P. C. Padhi*, Corrosion performance of naval brass in a simulated ocean water environment under different aqueous conditions, Mater. Chem. Phys., Vol. **326**, 2024, DOI: 10.1016/j.matchemphys.2024.129814.
26. *C.-H. Hsu, D.-Q. Ng, Y.-P. Lin*, Release of lead, copper, zinc from the initial corrosion of brass water meter in drinking water: Influences of solution composition and electrochemical characterization, Environ. Pollut., Vol. **352**, 2024, DOI: 10.1016/j.envpol.2024.124154.
27. *L. Yuan, C. Wang, R. Cai, Y. Wang, G. Zhou*, Spontaneous ZnO nanowire formation during oxidation of Cu-Zn alloy, J. Appl. Phys., Vol. **114**, 2013, DOI: 10.1063/1.4812569.
28. *X. Wang et al.*, Atmospheric corrosion of T2 copper and H62 brass exposed in an urban environment, Mater. Chem. Phys., Vol. **299**, 2023, DOI: 10.1016/j.matchemphys.2023.127487.
29. *V. N. Kalpana et al.*, Biosynthesis of zinc oxide nanoparticles using culture filtrates of Aspergillus niger: Antimicrobial textiles and dye degradation studies, OpenNano, Vol. **3**, 2018, DOI: 10.1016/j.onano.2018.06.001.
30. *A. N. Abu-Baker, L. A. Khalil, T. Al-Gonmeen*, A multi-analytical exploration of the chemical composition, microstructural properties and corrosion inhibiting treatment for an archaeological brass censer from Umm Zuwaytinah, Amman, Nucl. Instr. Meth. Phys. Res. B, Vol. **502**, 2021, DOI: 10.1016/j.nimb.2021.06.008.